Vibration-Based Methods for SHM

Claus-Peter Fritzen
Institute of Mechanics and Control Engineering – Mechatronics
and Center of Sensor Systems (ZESS)
University of Siegen
GERMANY

claus-peter.fritzen@uni-siegen.de

ABSTRACT

During the last years, the idea of a "smart" or "intelligent structure" has been extended from controlled structural systems to the field of Structural Health Monitoring (SHM), where sensor networks, actuators and computational capabilities are used to enable a structure to perform a self-diagnosis with the goal that this structure can release early warnings about a critical health state, locate and classify damage or even to forecast the remaining life-time. This paper intends to give an overview and point out recent developments of vibration-based methods for SHM. All these methods have in common that a structural change due to damage results in a more or less significant change of the dynamic behaviour. For the diagnosis an inverse problem has to be solved. We discuss the use of modal information as well as the direct use of forced and ambient vibrations in the time and frequency domain. Examples from civil and aerospace engineering as well as off-shore wind energy plants show the applicability of such SHM methods.

1.0 INTRODUCTION

Diagnosis and maintenance of technical structures nowadays is based mainly on periodic, scheduled inspections. Visual inspection, dye penetrant inspection, inspections with portable ultrasonic or eddy-current devices are the most common methods today. They are labor-intensive and time-consuming and the result depends strongly on the knowledge of the investigating expert. Disassembly of secondary parts is often required to get access to the important load bearing structural elements.

With the development of modern sensor technology, we try to adapt the idea of a biological nervous system to technical structures and make them smarter by installing a sensor network together with intelligent data processing to interpret the measurement data, see Figure 1. This information is directly available and can be sent as pre-warnings to the operator to prevent larger damage with extended repair or even catastrophic failure.

In the discussion about the benefit of Structural Health Monitoring (SHM), three aspects appear to be the most important : 1) reliability of safety-critical components to avoid disasters and prevent loss of life, 2) reliability under economic aspects, reducing financial losses caused by unproductive "down-time" (e.g. availability of aircrafts, power plants, etc.) and make inspection and maintenance more efficient, 3) change of design of light weight structures because the possibility of monitoring provides more information about the structure's current condition [1].

SHM methods are usually divided into local and global methods. This classification is based on the relation of the characteristic length of the waves or vibration pattern with respect to the defect size as well as to the overall structural dimensions. Local methods use e.g. high frequency ultrasonic waves whose wave lengths should be smaller than the size of the defect to be discovered. Therefore, the "hot spots" of the structure where damage is expected should be known. On the other hand, global methods typically use the lower modes of the structure as their "dynamic fingerprint". They can work with a much coarser sensor network which is usually distributed over the whole structure. In the latter case, it is not necessary that the sensors are located close to the damage site. For obvious reasons local methods can be expected to be more sensitive to incipient damage, however, the sensor instrumentation is more costly if large sensor arrays are required.

Rytter [2] defined 4 levels on the damage assessment scale: *Level I*: Damage detection; *Level II*: Damage localization; *Level III*: Damage quantification and *Level IV*: Prognosis of remaining service life. *Level I* only provides information that damage is present in the structure. For many practical applications this is absolutely sufficient. The challenge for future work on this level is the quantification and increase of the probability of detection (POD), get sensitive features and detect small damage in an early state without getting too many false alarms. Separating the effects resulting from damage from those coming from changes in environmental conditions is a further interesting topic. At *level II* the location(s) of single or multiple damage sites are determined. On *level III* the extent of damage is evaluated. For this purpose a model must be available to describe the effect of damage (by means of parameters like crack length, size of a delamination or stiffness decrease etc.) on the dynamic behavior. If no such model exists the damage metrics have to be determined by calibration experiments. Some authors [3,4] include the determination of the *type of damage* as an additional step between level II and III. The most sophisticated level is the step from diagnosis to damage prognosis and predictions of the remaining lifetime. This requires the combination of the global structural model with local damage models to predict the evolution of damage, e.g. fatigue crack growth, or probabilistic failure models [5,6]. Overviews can be obtained by [3,5,7-15]. However, the paper intends to discuss the basic physical ideas and show some recent trends of vibration-based methods.

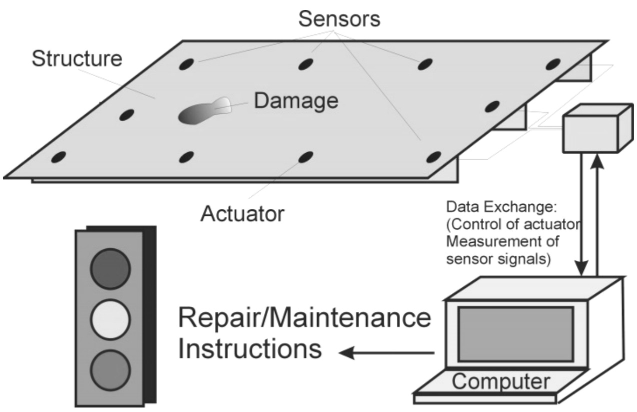

Figure 1: Smart Structure with self-diagnostic capabilities.

2.0 VIBRATION-BASED DIAGNOSIS OF STRUCTURES

2.1 Dynamical Model of Damaged Systems

We describe the dynamics of a general non-linear, time-varying, damaged structure by the spatially discrete and coupled system of the non-linear equation of motion (1) and the non-linear evolution of damage (2) in the following way:

$$\boldsymbol{M}(\boldsymbol{\theta}_d, \boldsymbol{\theta}_e, \boldsymbol{x}, t)\ddot{\boldsymbol{x}} + \boldsymbol{g}(\boldsymbol{x}, \dot{\boldsymbol{x}}, \boldsymbol{\theta}_d, \boldsymbol{\theta}_e, t) = \boldsymbol{f}_{op}(t) + \boldsymbol{f}_{Test}(t) \quad (1)$$

$$\dot{\boldsymbol{\theta}}_d = \boldsymbol{\Gamma}(\boldsymbol{\theta}_d, \boldsymbol{\theta}_e, \boldsymbol{x}, \dot{\boldsymbol{x}}, t) \quad (2)$$

$$\boldsymbol{y}(t) = \boldsymbol{h}_{out}(\boldsymbol{\theta}_d, \boldsymbol{\theta}_e, \boldsymbol{x}, \dot{\boldsymbol{x}}, t) \quad (3)$$

$$\boldsymbol{f}_{Test}(t) = \boldsymbol{h}_{in}(\boldsymbol{\theta}_d, \boldsymbol{\theta}_e, \boldsymbol{u}(t)) \quad (4)$$

where $\boldsymbol{M}$ is the mass matrix, $\boldsymbol{g}$ the force vector of elastic forces, damping forces, etc. depending on the displacements $\boldsymbol{x}$ and the velocities $\dot{\boldsymbol{x}}$ and t the time. The external load vector $\boldsymbol{f}$ is split into operational loads $\boldsymbol{f}_{\text{op}}$ and test loads $\boldsymbol{f}_{\text{Test}}$. The number of degrees of freedom (dof) is m. Equation (1) also allows to express non-linear effects of damage like stiffness variation due to an opening or closing crack depending on the instantaneous deformation [16]. The non-linear function $\boldsymbol{\Gamma}$ describes the evolution of the damage parameters $\boldsymbol{\theta}_d$ (e.g. crack length, play, loss of stiffness, loss of mass etc.). The parameter $\boldsymbol{\theta}_e$ in eqs. 1-4 indicates the influence of environmental and operational conditions (e.g. temperature, humidity, change of mass distribution, rotational speed, etc.) on the equation of motion. The two differential equations 1, 2 interact due to their coupling in the mechanical displacements, velocities and parameters. E.g. larger amplitudes of vibration $\boldsymbol{x}$ will cause larger stresses in the structure and hence increase the growth of damage. By means of eq. 2 it is possible to extrapolate into the future and by this perform a damage *prognosis* and estimate the *residual service life* [17,18]. Due to the statistical variations in the measurements (e.g. S-N curves), assumptions and uncertainties about the future loads and damage growth models (Paris law of crack propagations, linear damage accumulation rule according to Palmgren-Miner, etc.), the estimation of the remaining life-time is of probabilistic nature and not a purely deterministic problem. A compilation of different methods for modeling the change of stiffness of structural elements due to damage is presented e.g. in [19].

The evolution of the damage on one hand and the dynamics of the structure on the other hand usually takes place on two different time scales. Compared to the vibrations of the structure the evolution of damage (fatigue, corrosion, etc.) is usually considered to be a rather slow process so that we can assume that $\boldsymbol{\theta}_d$ keeps constant during the short time span of the data acquisition. An exception from this is impact damage, where the damaging event takes place in a very short moment. Model-based methods require accurate computational models. Thus, model-updating [20,21] is an important step to improve the quality of the model before it is used for damage identification.

Eq. 3 delivers a relation between the internal model state variables (displacement, velocities) and parameters with the output variables $\boldsymbol{y}$(t) like strains, voltages, accelerations, etc. which we wish to compare with a corresponding output of a measurement device. The fourth equation describes the transformation of an input signal $\boldsymbol{u}(t)$ (e.g. a voltage) into forces or moments, e.g. in the case of piezo-actuators. In eq. 3, 4, the damage parameters $\boldsymbol{\theta}_d$ can also include sensor or actuator failure.

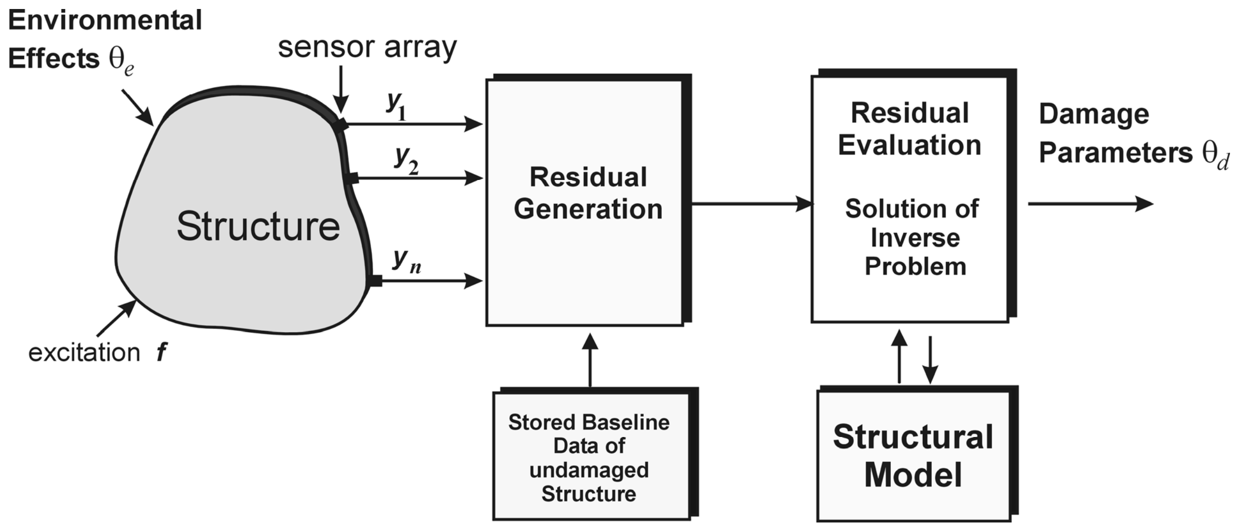

Figure 2: Inverse problem: from measurement to damage evaluation.

2.2 Inverse Problem

The deviation of the outputs $\Delta\boldsymbol{y} = \boldsymbol{y} - \boldsymbol{y_0}$ from a reference signal $\boldsymbol{y}_0$ (the baseline, representing the undamaged system) due to changes of the damage parameters $\boldsymbol{\theta}_d$ can be used for diagnosis. While the forward problem is $\Delta\boldsymbol{y} = \boldsymbol{F}(\boldsymbol{\theta}_d, \boldsymbol{\theta}_e)$ the inverse problem can be written as $\boldsymbol{\theta}_d = \boldsymbol{F}^{-1}(\Delta\boldsymbol{y}, \boldsymbol{\theta}_e)$, see Figure 2. Generally this represents an inverse task with all the problems that can arise like non-uniqueness of the solution in case of incomplete information of the measurement data or unstable solutions due to measurement noise. Very often the deviations of the time signals $\boldsymbol{y}$, $\boldsymbol{y}_0$ are not used directly, but an intermediate step is introduced to extract characteristic features of the system such as modal data, FRFs, etc. This condenses the information to a lower dimensional space. Minimization of the residuals leads to a linear or a non-linear optimization task, depending on the formulation of the residuals. In addition, constraints can be introduced.

2.2.1 Pattern Recognition and Neural Networks

Damage assessment can also be considered under the aspect of a pattern recognition task [4,22,24-28]. The cause-effect relation of damage and changes in the dynamical behavior (features) can be mapped by neural networks (NN) which are trained to given input and output vectors. This approach is called supervised learning [23]. The output targets represent different damage scenarios while the input patterns represent the corresponding features from the dynamic behavior such as deviations of the eigenfrequencies and mode shapes from the undamaged state. These changes can be determined from calculations, simulating different damage scenarios or by real data from real damage cases if available. Alternatively, other features such as wavelet coefficients [27] etc. can be used. The generation of the training pattern using a model makes clear that we may run into the same problems as with the inverse problem if we do not have an accurate structural model. Contrary to that, unsupervised learning [23] does not make use of labeled training data. Instead we have a collection of unlabeled samples and we try to classify them based on the features in the data only.

2.2.2 Influence of Environmental Conditions

It is well-known that environmental effects, represented by the parameters $\boldsymbol{\theta}_e$ (like temperature, humidity etc.), can have a strong influence on the dynamics of the vibrating system (by changing stiffness, damping and mass properties), the working conditions of the sensors and actuators (e.g. material properties of piezo-electric elements, properties of adhesives, etc.) but also on the evolution of the damage, e.g. by corrosion. Concerning the first two aspects, it is important that we can separate the dynamic effects caused by the environmental parameters $\boldsymbol{\theta}_e$ from the changes caused by damage parameters $\boldsymbol{\theta}_d$. Otherwise, we are not able to come to a reliable decision. As many studies have shown, changes caused by temperature can be easily of the same order or higher compared to the changes caused by damage. The compensation of the environmental effects, namely temperature, is considered to be one of the major topics today and is essential for the success of the diagnosis. One solution is to provide a data base of multiple reference states for different environmental conditions, e.g. different temperature levels [29]. To find optimal reference points, in [30,37] clustering methods have been applied.

Other methods for compensation of the effects of changing environmental conditions were developed by Sohn et al. using a combination of AR-ARX (AR models with exogenous inputs) models with Non Linear Principal Component Analysis (NLPCA) [31]. Kullaa uses missing data analysis [32] or factor analysis [33,34] to eliminate the environmental effects from damage sensitive features. Yan et. al [35] propose a local PCA for structural damage diagnosis under changing environmental conditions. A review of methods for compensation of environmental conditions can be found in [36].

2.2.3 Sensor Distribution

The damage identification result depends strongly on how many sensors can be used, the location of these sensors and which kind of sensors are used, but also on the frequency spectrum of the sensor signals. The accuracy of the solution of the inverse problem $\boldsymbol{\theta}_d = \boldsymbol{F}^{-1}(\Delta \boldsymbol{y}, \boldsymbol{\theta}_e)$ depends on the amount of information we can gather from the measurement data. Of course we want to maximize this information, resp. to minimize the uncertainty of the damage parameters θ_d. Practically, this means that we wish to obtain parameter values with low variance. A measure for uncertainty is the information entropy [38]. Papadimitriou et. al. [38] show that minimizing the entropy is equivalent to maximizing the determinant of the Fisher information matrix containing the derivatives of the measured responses with respect to the parameters θ_d: $\partial y_i / \partial \theta_{dj}$. The derivatives represent the sensitivity of the responses with respect to the various damage parameters. Furthermore, the inverse Fisher information matrix represents the lower bound of the parameter variances (known as Cramer-Rao lower bound). From that it is clear that we should select sensors which maximize the determinant of the Fisher matrix. For the selection of appropriate sensor locations for damage identification with modal data, in [39,40] an efficient forward-backward selection procedure is proposed. Li [41,42] investigates the sensor distribution under the aspect of optimal, independent vibration mode determination for SHM.

Usually, the more sensors we use, the larger is the information, however, from a certain point this is impractical for economic reasons. Moreover, the addition of a new sensor does not necessarily guarantee that the information is increased significantly, it may happen that the information of the new sensor is already included in the other sensor signals. A measure for the redundancy of information is the Mutual Information [43]. At the first glance, redundancy looks like a waste of resources, however under certain aspects of sensor fault detection, we can make use of this redundancy, see next section.

2.2.4 Sensor Fault Detection

This research topic has been paid more attention during the last years. It has been recognized as an important issue in SHM that failure of one or more sensors could lead to a point where the whole SHM system -at least temporarily- might become useless. In the ideal case we assume that the sensors should have a longer life-time than the structure they have to monitor but in practice, however, especially under harsh conditions, the sensors themselves have a limited life expectation. Sensor faults can be classified after its types as: bias, complete failure, drifting and precision degradation [44].

Identification of faulty sensors and reconstruction of the faulty sensor signals have been studied e.g. by Dunia et al. [44] and Kerchen et al. [45] using the principal component analysis (PCA). Mattern et al. [46] used neural networks and Worden [47] combined auto-associative neural networks (AANN) with autoregressive models with exogenous inputs (ARX). Kullaa [48] used a so-called missing data analysis. A mutual information concept and AR models have been proposed by Kraemer and Fritzen [49] to identify faulty sensors in vibrating systems. Most of these methods make use of redundant information of the different sensor signals to find out the damaged sensor. Sensor faults of piezo-electric elements can be tested using their self-sensing properties and comparing the admittance of the sensor [50,75,76] with a reference state.

3.0 DAMAGE IDENTIFICATION FOR LINEAR SYSTEMS

Let us assume that the dynamics of the structure can be described by the linear equation of motion with m degrees of freedom

$$\boldsymbol{M}\ddot{\boldsymbol{x}} + \boldsymbol{C}\dot{\boldsymbol{x}} + \boldsymbol{K}\boldsymbol{x} = \boldsymbol{f}(t) \qquad (5)$$

where $\boldsymbol{M}$, $\boldsymbol{C}$ and $\boldsymbol{K}$ are the $m \times m$ mass, damping and stiffness matrix, respectively. $\boldsymbol{x}$ is the displacement vector and $\boldsymbol{f}$ again represents the external load. If the system is undamped or only lightly damped characteristic features of the system are the natural frequencies ω_i (eigenvalues $\lambda_i = \omega_i^2$) and the (real) normal modes $\boldsymbol{\varphi}_i$ determined by the solution of the eigenvalue problem

$$\left(\boldsymbol{K} - \omega_i^2 \boldsymbol{M}\right)\varphi_i = \boldsymbol{0}\,. \tag{6}$$

A widely used approach is to introduce correction parameters which represent the model changes in the system matrices on a substructure or element level:

$$\Delta\boldsymbol{K} = \sum_j \boldsymbol{K}_j \Delta a_j\ ;\ \ \Delta\boldsymbol{C} = \sum_j \boldsymbol{C}_j \Delta a_j\ ;\ \ \Delta\boldsymbol{M} = \sum_j \boldsymbol{M}_j \Delta a_j\,. \tag{7}$$

The general damage parameters $\boldsymbol{\theta}_d$ are replaced by a simpler approach of linear matrix correction parameters $\Delta\boldsymbol{a}$. The determination of the unknown correction parameters which localize and quantify the damage can be done by solving the inverse problem, minimizing the weighted sum of the components of the data error $\boldsymbol{\varepsilon}$ and constraining the norm of the parameter vector $\boldsymbol{\Delta a}$ to “small” values, we get the extended weighted least squares (EWLS) functional [12]

$$J = \boldsymbol{\varepsilon}^T \boldsymbol{W}_\varepsilon \boldsymbol{\varepsilon} + \Delta\boldsymbol{a}\boldsymbol{W}_a \Delta\boldsymbol{a} \qquad \text{with} \qquad \boldsymbol{\varepsilon} = \boldsymbol{S}\Delta\boldsymbol{a} - \boldsymbol{r}\,. \tag{8}$$

Minimizing J with respect to the components of $\boldsymbol{\Delta a}$ yields the linear equation system

$$(\boldsymbol{S}^T \boldsymbol{W}_\varepsilon \boldsymbol{S} + \boldsymbol{W}_a)\boldsymbol{\Delta a} = \boldsymbol{S}^T \boldsymbol{W}_\varepsilon \boldsymbol{r} \tag{9}$$

The vector $\boldsymbol{r}$ represents the changes of the measurement data (different types are discussed in the following sections). $\boldsymbol{S}$ is the corresponding sensitivity matrix following directly from the derivation or has to be calculated by the first order partial derivatives of the dynamic quantities with respect to the parameters $\boldsymbol{a}$. $\boldsymbol{W}_\varepsilon$ and $\boldsymbol{W}_a$ are appropriate positive definite weighting matrices. With $\boldsymbol{W}_a = \gamma \cdot \boldsymbol{I}$, Eq. 9 can be considered as Tikhonov regularization method, where γ is a scalar factor and $\boldsymbol{I}$ is the identity matrix. [51] has derived an iterative version of the Tikhonov method. Link [52] has presented an interesting multi-model approach adapting the model of the undamaged and damaged system simultaneously. There is a certain disadvantage of minimizing the second term in Eq. 8 in the context of damage localization: due to the quadratic nature, the algorithm prefers to change many parameters with small changes instead of minimizing only few parameters with larger changes. For this reason special attention has to be paid to the problem of the high dimensionality of the parameter space, which has to be reduced as far as possible [7,53,54]. The reduced subset of the dominant parameters must be able to describe the damage scenario and should finally concentrate on those parameters corresponding to the damaged sub-region(s) of the structure. The parameter reduction strategy is performed in two steps as described in [54]. As result only those parameters are considered which yield a significant contribution to reduce the equation error $\boldsymbol{\varepsilon}$.

3.1 Modal-based Approaches to Damage Identification

Modal quantities can be extracted by means of classical modal analysis methods using output measurements resulting from special input test signals [20,55,56] or by output-only methods which use the ambient excitation from wind, traffic loads, etc. [57,58]. The use of modal data for system identification is discussed by Natke [20] or Friswell and Mottershead [21] and assumes linearity of the structure.

3.1.1 Eigenfrequency and Mode Shape Residuals

The first approaches used the resonant frequencies of a structure only, e.g. [59]. A stiffness change produces a characteristic shift of the eigenfrequency spectrum $\boldsymbol{r}_{\lambda i} = \Delta\omega_i^2 / \omega_i^2$, $i = 1,2,\cdots$ which are used to deduce the parameters causing this change. Usually the higher frequencies are more sensitive and show larger shifts. Expressing the residuals as relative changes, it can be observed that they are more or less of the same order. Problems using eigenfrequencies alone arise in the case of symmetric structures or if the two spectra cannot be assigned properly. Further problems appear if the eigenfrequency changes are so small that effects due to damage are masked by the changes due to environmental conditions. These changes alone do not allow to draw conclusion about the source of the frequency changes. Therefore a model must be available that "knows" the relation between frequency and stiffness changes. The model allows also to calculate the first order partial derivatives describing sensitivities of the eigenfrequency with respect to parameter changes, see [20,21].

The mode shapes introduce spatial information about the damage. Local stiffness changes result in a local change of the mode shapes curvature and hence in the mode shapes themselves. For a mode no. *i* ("d" denotes damaged, "0" the reference state) the change of the eigenvector is $\boldsymbol{r}_{\varphi i} = \varphi_{d,i} - \varphi_{0,i}$.

Correct pairing of the eigenvalues/eigenvectors and correct scaling of the mode shapes is solved by applying the Modal Assurance Criterion (MAC) and the Modal Scale Factor (MSF), see e.g. [7,21,56]. From the author's point of view using both frequencies *and* mode shapes simultaneously is preferred. The modal sensitivities can be determined by the methods of Fox and Kapoor or by Nelson, see [21] for a compilation. Higher mode shapes are more sensitive to local parameter changes, however problems may arise from the sensor distribution: the sensor network has to be dense enough to properly describe the mode shape and to avoid spatial aliasing. Furthermore, it is more difficult to accurately calculate the higher frequencies and mode shapes from the mathematical model.

3.1.2 Modal Force Residuals

Another type of residual is the Modal Force Residuals which can be defined by putting the measurement data ω_i , $\boldsymbol{\varphi}_i$ into the eigenvalue problem:

$$\left(\boldsymbol{K}_0 - \omega_{i,d}^2 \boldsymbol{M}_0\right)\boldsymbol{\varphi}_{i,d} = \boldsymbol{r}_{MFR,i} = -\Delta\boldsymbol{K}\varphi_{i,d} . \tag{10}$$

With the corrected stiffness matrix $\boldsymbol{K}_d = \boldsymbol{K}_0 + \Delta\boldsymbol{K}$ (the mass matrix is assumed to be unaffected by the damage, "0" indicates the reference system, "*d*" damaged). Eq. 7 connects the change of the stiffness matrix $\Delta\boldsymbol{K}$ with the correction parameters Δa_j . In practice not all dofs of the model can be measured so that $n_m << m$. We have to expand the shorter measurement vector to the full model size of *m* by the transformation $\varphi_{i,d,expd} = \boldsymbol{T}_\omega \varphi_{i,d,meas}$ using an appropriate (frequency dependent) transformation matrix $\boldsymbol{T}$. Expansion methods are discussed e.g. in [7,21]. The expansion can introduce additional errors, furthermore this method is sensitive to measurement errors. It can be observed that Least Square solutions without parameter selection strategies tend to spread the parameter changes over the whole parameter vector instead of focusing on a few significant parameters. Therefore, Zimmermann developed an alternative approach, the Minimum Rank Pertubation Technique (MRPT), to determine the minimum-rank change of the stiffness matrix [60]. Modal force residuals are used with expansion of the mode shape vectors. A detailed derivation can be found in [60]. This method has also been applied by Zimmerman et al. to FRFs and also so-called Ritz-vectors, see [61].

3.1.3 Energy Considerations and Curvature Mode Shapes

Stubbs, Kim and Farrar [62] developed a formula from strain energy expressions to determine a change of the bending stiffness *EI* due to damage in a flexible beam or beam-like structures. Each element/substructure is tested to discover a local change of the bending stiffness. The change-coefficients are determined by means of the local curvatures (second derivatives) of the mode shape functions for the reference state "0" and the damaged state "d". Maeck [63] uses a regularization technique to reduce the errors from the numerical curvature calculation. A more general approach was presented by Ladeveze and Reynier [64] with the MECE concept (Minimization of the Error in the Constitutive Equations). As a result they also get indicators from strain energy expression pointing out the most erroneous locations of the reference model. These locations indicate the changes due to damage. A sensitivity-based approach in connection with modal kinetic energies (MKE) was proposed in [40,65].

3.2 Frequency Domain Methods Based on Forced Vibrations

Instead of first extracting the modal parameters from forced vibration or Frequency Response Function (FRF) measurements, it is possible to use these measurement data, eq. 11, directly for damage identification [20,21,53]. Transforming Eq. 5 into the frequency domain delivers the complex algebraic equation as further basis

$$\left(-\Omega^2 \boldsymbol{M} + i\Omega \boldsymbol{C} + \boldsymbol{K}\right)\boldsymbol{X}(\Omega) = \boldsymbol{F}(\Omega) \tag{11}$$

The output error compares the frequency domain responses of the damaged with the undamaged system directly. For any frequency (index ν) we get the complex deviation $\boldsymbol{r}_O(\Omega_\nu) = \boldsymbol{X}_d(\Omega_\nu) - \boldsymbol{X}_o(\Omega_\nu)$ which can be arranged for all ν (and possibly for other force configurations) in one big vector $\boldsymbol{r}$. During the iterative minimization of eq. 8 problems with the convergence may arise, because the shifts of the resonant peaks can cause very large deviation in the cost function.

Similar to the modal force residual method, the Input Residual Method (IRM) uses the mistuning of the equation of motion when the measurement data do not match the model represented by "0"-system matrices. For any frequency index ν we get the complex input residual

$$\boldsymbol{r}_I(\Omega_\nu) = \boldsymbol{F}_d(\Omega_\nu) - \left(-\Omega_\nu^2 \boldsymbol{M}_0 + i\Omega_\nu \boldsymbol{C}_0 + \boldsymbol{K}_0\right)\boldsymbol{X}_d(\Omega_\nu) \tag{12}$$

which finally leads to a *linear* relation between $\boldsymbol{r}_I$ and the parameters Δa_j. In the case of incomplete measurement the dynamic response $\boldsymbol{X}$ has to be expanded to the full size of the model as before which is however a source of errors. Furthermore the IRM is sensitive to measurement noise. Further details are described in [7].

Oeljeklaus [66] has presented an interesting approach called Projected Input Residual Method (PIRM) to overcome the problem of incomplete measurement data. The intention is to take advantage of the nice properties of the input residual method, especially the convexity of the cost function ensuring convergence to the minimum. This is reached by the introduction of a special projection matrix which is constructed in a way to mask out the lacking components of the response. Expansion is not required here for the PIRM.

When using FRFs [53], the input or output errors can be formulated quite similar as shown in the forced vibration section, simply replacing the force input by the identity matrix $\boldsymbol{I}$ and the outputs $\boldsymbol{X}$ by the FRF matrix $\boldsymbol{H}$. Usually, not the full FRF matrix is required. In this case only one or more columns of the $\boldsymbol{H}$ matrix are used as well as the corresponding columns of the $\boldsymbol{I}$ matrix. It is well-known that the FRFs (and the forced vibration as well) can be represented by means of the structure's modal data and therefore they use the same physical information about the system.

3.2.1 Transmissibility Ratios

The transmissibility ratios (TR) are defined as the ratio of two Fourier transformed output signals X_i and X_j . i and j denote different responses obtained from different sensor positions/directions,

$$T_{ij}(\Omega) = \frac{X_i(\Omega)}{X_j(\Omega)}, \tag{13}$$

They also can be used in the case of ambient vibration with output-only measurements if the different channels are measured simultaneously. For random signals a formulation based on spectral densities can be used instead [67]. Johnson and Adams [68] showed that the representation of the response by its zeros and poles is very useful. The poles which appear in all responses and which are influenced by all parameters of the system are eliminated when calculating the transmissibility ratio. Only the zeros remain in the equation, so that the changes of the TRs can be used for damage localization, [69]. Hilson et al. [70] used the transmissibility ratios to train neural networks for pattern recognition.

3.2.2 Electro-Mechanical Impedance Method (EMIM)

The impedance method works in the higher frequency range (typically > 30 kHz). At high frequencies, the structural resonances are localized and highly sensitive to local damage. Structural changes due to damage are observed by changes in the impedance spectrum of the electro-mechanical system. A detailed overview on the EMIM is given in [71,72,73,74]. Practically the impedance of the EM-system is determined by the input voltage and the output current through the piezo-electric actuator: $Z_{EM}(\Omega) = V(\Omega)/I(\Omega)$ at a certain frequency Ω, see Figure 3. By this, we make use of the self-sensing properties of the piezo-element which is sensor and actuator at the same time. A frequently used piezo-electric material is lead zirconate titanate (PZT). The idea is that the damage in the structure changes the structural impedance and hence the resulting impedance spectrum of the coupled EM-system: $Z_{EM} = f(Z_{Struct}, Z_{PZT})$:

$$\frac{V(\Omega)}{I(\Omega)} = Z_{EM}(\Omega) = \frac{1}{i\Omega C}\left(1 - \kappa^2 \frac{Z_{struct}(\Omega)}{Z_{PZT}(\Omega) + Z_{struct}(\Omega)}\right)^{-1} \tag{14}$$

where C is the zero load capacitance and κ is an electro-mechanical cross coupling coefficient of the piezo-electric transducer, Z_{struct}, Z_{PZT} are the impedances of the structure and the piezo-element, respectively. Usually, the real part of the actual spectrum is compared to the stored reference spectrum $Z_{EM,0}$ of the undamaged system. Level I-detection can be performed. The impedance method is a qualitative method and possesses a local character. At high frequencies, the structural resonances are localized and highly sensitive to local damage. Furthermore the actuator energy is dispersed into the structure so that effects from the damage can be seen only closely to the actuator position allowing also Level II diagnosis. The EMIM is also well-suited for the self-diagnostics of the piezo-elements, see e.g. [50,75,76]. In this case we are not primarily interested in detecting structural damage but in detecting slow degradation and abrupt malfunctioning of the sensor system.

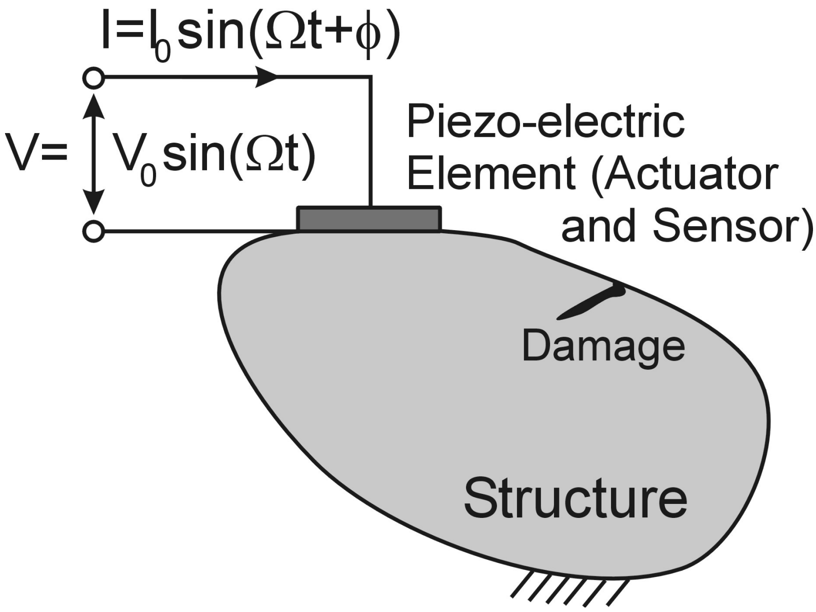

Figure 3: Measurement of the impedance of the coupled electro-mechanical system from voltage and current.

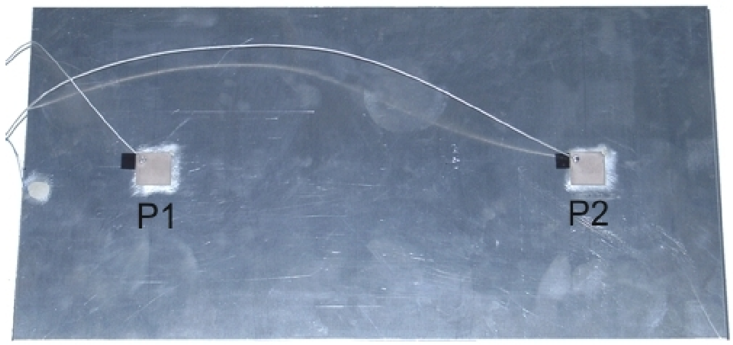

Figure 4: Aluminium plate with two quadratic piezo-electric elements.

The reciprocal complex value of the impedance is called admittance:

$$Y(\Omega) = 1 / Z_{EM}(\Omega) \tag{15}$$

A typical example for an admittance spectrum is shown in Figure 5, here the imaginary part, the so-called susceptance, is displayed. Own experiments have been carried out to explore the changes of the admittance spectra due to environmental influences due to temperature θ_e and also due to different types of damage θ_d . In this case, the figure shows the degradation effects of the adhesive layer between the PZT-element and the structure. The left part of the spectrum (for lower frequency values) is characterized by a linear curve with slope C (the capacitance of the piezo-element) increasing with frequency Ω, compare to eq. 14. Resonance of the piezo-element itself characterizes the middle part of the curve. A modelling approach of the system of PZT-element/adhesive/structure to better understand its behavior of the can be found in [75,76]. By means of machine learning, it is possible to distinguish between environmental effects and damage.

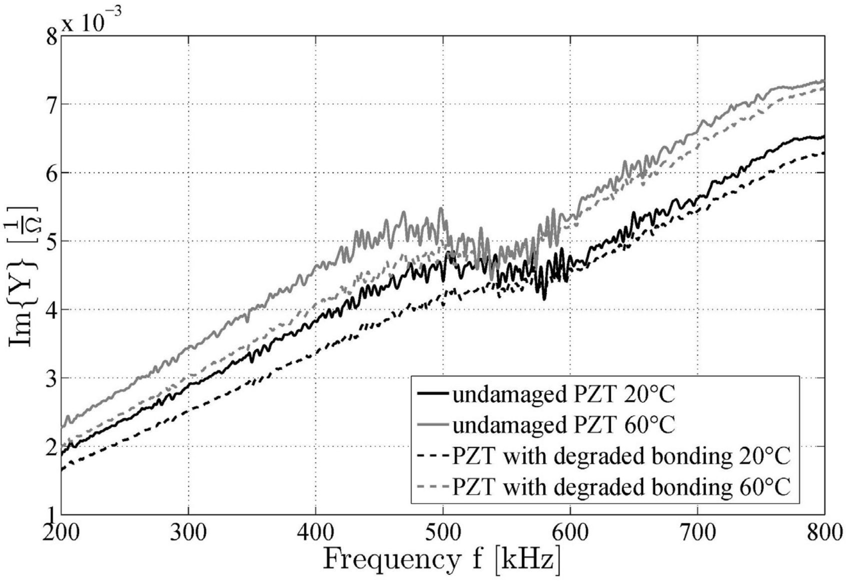

Figure 5: Measured Admittance Spectra for a PZT element on an aluminium plate under different temperature and health conditions.

3.3 Time Domain Methods

The formulation of the diagnosis problem in the time domain especially in state space notation is frequently used in control and automation theory to identify faults in general technical systems [77]. These ideas have also been used in the context of structural diagnosis and vibration problems. Fassois [78] gives an overview on time-domain methods. Some representatives are discussed in the following sections.

3.3.1 Nullspace-Based Fault Detection Method (NSFD)

Basically this method has been developed by Basseville et al. [79,80]. It is a Level-I method and works under *output-only* conditions assuming that the system excitation is random Gaussian white noise. However, practical experience shows that the method yields good results also under less restrictive conditions. The system dynamics are represented as discrete time state space formulation with unknown random input $\boldsymbol{w}(k)$ and outputs $\boldsymbol{y}(k)$:

$$\boldsymbol{z}(k+1) = \boldsymbol{A}\,\boldsymbol{z}(k) + \boldsymbol{w}(k) \tag{16}$$

$$\boldsymbol{y}(k) = \boldsymbol{C}\,\boldsymbol{z}(k) + \boldsymbol{v}(k) \tag{17}$$

where $\boldsymbol{v}(k)$ denotes the measurement noise, $\boldsymbol{A}$ and $\boldsymbol{C}$ are the system and the measurement matrix, respectively and $\boldsymbol{z}$ is the state space vector. The stochastic responses $\boldsymbol{y}$ are used to calculate the Hankel matrix. The first step is to determine the covariances of $\boldsymbol{y}$: $\boldsymbol{R}_j = E\left(\boldsymbol{y}(k+j)\boldsymbol{y}^T(k)\right)$, they can be estimated from the sampled outputs $\boldsymbol{y}(k)$. The block Hankel matrix $\boldsymbol{H}$ is:

$$\boldsymbol{H}_{\alpha,\beta} = \begin{bmatrix} \hat{\boldsymbol{R}}_1 & \hat{\boldsymbol{R}}_2 & \cdots & \hat{\boldsymbol{R}}_\beta \\ \hat{\boldsymbol{R}}_2 & \hat{\boldsymbol{R}}_3 & \cdots & \hat{\boldsymbol{R}}_{\beta+1} \\ \vdots & \vdots & \ddots & \vdots \\ \hat{\boldsymbol{R}}_\alpha & \cdots & \cdots & \hat{\boldsymbol{R}}_{\alpha+\beta-1} \end{bmatrix}; \text{with } \hat{\boldsymbol{R}}_j = \frac{1}{n_t - j - 1} \sum_{k=1}^{n_t - j} \boldsymbol{y}(k+j)\,\boldsymbol{y}^T(k). \tag{18}$$

n_t is the number of data samples per sensor and j is the time shift. α and β determine the maximum number of time shifts. The Damage Indicator value is defined as

$$D_{NSFD} = \boldsymbol{\zeta}^T \hat{\Sigma}^{-1} \boldsymbol{\zeta} \quad \text{where} \quad \boldsymbol{\zeta} = vec\left(\boldsymbol{S}^T \boldsymbol{H}_{\alpha,\beta}\right) \tag{19}$$

is the residual vector. $\hat{\Sigma}$ is an estimate of the residual covariance matrix. $vec(\ldots)$ is the stack operator returning a vector whose elements are taken column-wise from the original matrix. The column vectors of the matrix $\boldsymbol{S}$ span the null space (or left kernel space) of the Hankel matrix so that $\boldsymbol{S}^T \boldsymbol{H}_{\alpha,\beta} = \boldsymbol{0}$. $\boldsymbol{S}$ can be obtained by means of a *SVD* of the Hankel matrix and is stored as information about the undamaged system. If new measurement data are taken from the undamaged structure and the Hankel matrix is composed of the data of the undamaged system, the residual $\boldsymbol{\zeta}_n$ (*n* being a current number of measurement data set) should be close to zero and vary only within certain statistical bounds due on the measurement errors. If damage occurs, ζ_n should differ significantly from zero. For a more detailed discussion of the method see [79,80], an applications of the theory within the smart structures concept is described in [81,82]. In [82] it was shown by controlled experiments in an oven how changes of the system response due to temperature variations can be compensated and still lead to reliable damage indication even under strong temperature variation. In [83] different formulations of the NSFD method are compared to principal component analysis (PCA).

3.3.2 Residual Generation Using Kalman Filters and Time Series Models

The idea using Kalman Filters (KF) for damage detection is to first identify a multi-input multi-output state space model from measured reference data sets and then to determine the corresponding Kalman gain matrix. When applying new data sets to the KF, it produces residuals (or also called innovations in the KF context) by testing the nominal model against these new measurement data sets. If the actual data set stems from a damaged system, however the KF was designed for the reference model, the misfit shows up in a change of the statistical properties of the residuals. This change can be used to perform a detection that a change of the mechanical structure has occurred (Level I). First, this method was presented in the automation literature, e.g. [84]. In [85] the KF was applied to detect a delamination in a CFRP plate. In [16], an Extended Kalman Filter (EKF) was used to determine the crack depth of an opening and closing crack in a rotating shaft exhibiting nonlinear dynamic behavior.

Sohn et al. [22] have demonstrated the use of the Auto-Regressive (AR) and AR with Exogenous input (ARX) time-series models in a two-stage procedure which is quite similar to the KF approach. Here, the basic idea is to identify an ARX reference model from data sets of discrete time series representing the undamaged structure in a first stage. This model represents the dynamic behavior of the undamaged system (reference state). In the second stage this model is tested with new data sets. The resulting residual error is statistically evaluated. As long as the feature extracted from the residuals lies within a defined range of the statistical variation there is no evidence that the structure has changed its physical properties. The ratio $\sigma(\varepsilon_y)/\sigma(\varepsilon_{y0}) > h$, $h > 1$, is defined here as damage sensitive feature where σ is the standard deviation of the residual time series. ε_{y0} is the residual error after fitting the ARX model in stage I, ε_y is the residual error testing ARX model against the current data sets in stage II. This method provides a Level *I* test. An appropriate threshold for *h* has to be chosen. Further aspects of outlier analysis are discussed [22].

4.0 EXAMPLES

4.1 Z24-Bridge: Use of Modal Data from Ambient Vibrations

Figure 6: Z24-bridge (Photo: KU Leuven).

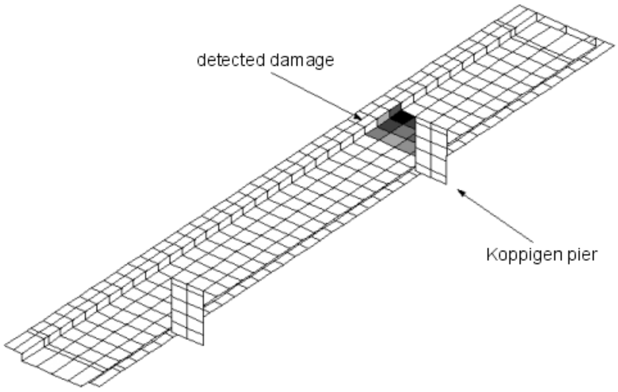

Figure 7: Visualization of calculated damaged zone: stiffness loss indicated by the darker elements determined with the modal kinetic energy method.

The Z24-bridge was a 60m long, three-span pre-stressed concrete girder bridge with two lanes crossing the Swiss highway A1, Figure 6. This bridge was provided by the Swiss road traffic authorities for the European SIMCES project (System Identification to Monitor Civil Engineering Structures) for extensive investigations on monitoring using vibration-based methods. During the project different kinds of damage had been introduced. As a benchmark example this bridge was also investigated during the EU COST F3 action "Structural Dynamics" [86-88]. A scenario of great practical relevance is the dangerous undercutting of a pier, a hardly detectable damage that frequently appears in reality. The settlement of the "Koppigen pier" of 9.5 cm caused an overload in the bridge which resulted in cracks at the connection between the pier and the girder box. The model-based approach requires a computational model. For the model-updating process a reference set of five eigenfrequencies and real mode shapes was identified from "output-only" measurement data [57-58]. The finite element model shown in Figure 7 consists of 650 shell elements and approximately 3800 dofs, [65]. The updating parameters $\boldsymbol{p}$ were the stiffnesses of the springs that have been used to model the boundary conditions (bridge bearings and connection of the piers to the ground) as well as the Young's modulus of the bridge material and the pier material. The used objective function J contains a certain number (here n_{modes}=5) of measured (lower index *meas*) and simulated (lower index *mod*) eigenfrequencies ω and the corresponding mode shapes.

$$J(\boldsymbol{p}) = \sum_{i=1}^{n_{modes}} w_{\lambda,i} \left(\frac{\omega_{i,meas}^2 - \omega_{i,mod}^2(\boldsymbol{p})}{\omega_{i,meas}^2} \right)^2 + \sum_{i=1}^{n_{modes}} w_{MAC,i} \left(1 - MAC_{i,i}(\boldsymbol{p})\right)^2 \tag{20}$$

The relative difference between the eigenfrequencies and the correlations between the mode shapes (by help of **M**odal **A**ssurance **C**riterion, *MAC*) in eq. 20 are weighted by w_λ and w_{MAC} respectively. The results of model updating are displayed in and Table 2. More details can be found in [65].

Table 1: Comparison of eigenfrequencies.

	Mode 1	Mode 2	Mode 3	Mode 4	Mode 5
Meas. [Hz]	3.9	5.0	9.8	10.3	12.7
Model [Hz]	3.9	5.3	9.8	10.4	12.0

Two model-based damage identification procedures, the Inverse Eigensensitivity method and the Modal Kinetic Energy method have been applied. They both use frequencies and mode shapes as input, however in a different way. The experimental modal data have been extracted from output-only measurement data after the bridge was damaged.

Table 2: MAC-values for measured and simulated mode shapes.

MAC-values [%]		Model							
		Mode 1	Mode2	Mode 3	Mode 4	Mode 5	Mode 6	Mode 7	Mode 8
Meas.	Mode 1	**99.6**	0.0	0.0	0.0	0.2	0.0	0.0	0.0
	Mode 2	0.1	**97.0**	1.6	1.0	0.0	0.0	0.6	0.2
	Mode 3	0.2	3.0	**96.2**	2.9	0.2	0.3	0.5	0.0
	Mode 4	0.0	2.3	4.9	**94.8**	0.2	1.1	0.7	0.4
	Mode 5	0.0	0.2	0.1	0.3	**91.4**	0.0	0.6	0.2

The simulated undercutting of the pier produced cracks on the lower side of the bridge near the pier leading to a reduced stiffness in this bridge section. Figure 7 shows that the stiffness reduction can be successfully identified by the energy method. The gray elements in Figure 7 illustrate the identified location of damage: the darker the color, the higher the indicated stiffness loss (the intensity of damage). The Inverse Eigensensitivity Method using frequencies and mode shapes yields a very similar result, see [65].

4.2 Airplane Fuselage Structure

This example shows a stiffened shell structure with stringers from the airplane Airbus A320. The purpose was to find out whether damage in the stringers can be detected and localized. The method used here is a combination of the self-sensing capabilities of the piezo-elements (as usually used for the impedance method) and the evaluation of the output voltages using the NSFD method, see [89] for more details. The structure was excited and measured consecutively with nine PZT elements (P1 to P9, see Figure 8). Each PZT element is acting as actuator and sensor according to the self-sensing principle. The positions of the sensors are displayed in Figure 8. The system was excited by a sweep signal in a frequency range of 10-20 kHz. The time period for each measurement is 10 s. The total number n_m of measurements for each PZT was 15, 10 for the undamaged and 5 for the damaged state of the structure. Damage, see Figure 8, was introduced into one of the stringer of the shell structure between PZT el. no. 9 and 6, but closer to PZT 9. PZT elements no. 9, 6 and 3 are placed also on the same stringer.

The NSFD-Method, see Eq. (14) and (15) , was applied only for the output signals for each sensor separately. The results are displayed in Figure 9. The NSFD localized the damage correctly close to the sensor 9 in measurements 11 to 15. The next highest change in the damage indicator D_m (see eqn. 6) was found by sensor 6, also during the measurements 11-15 (meas. with damage), which is the neighbor of sensor no. 9. The application of ARX models yielded quite similar results with a significant change for sensor 9.

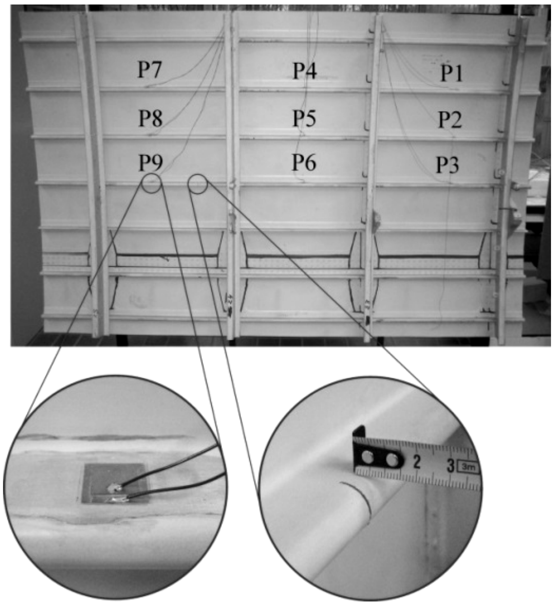

Figure 8: Stiffened shell structure with piezo-element on stringers and damage close to PZT no. 9.

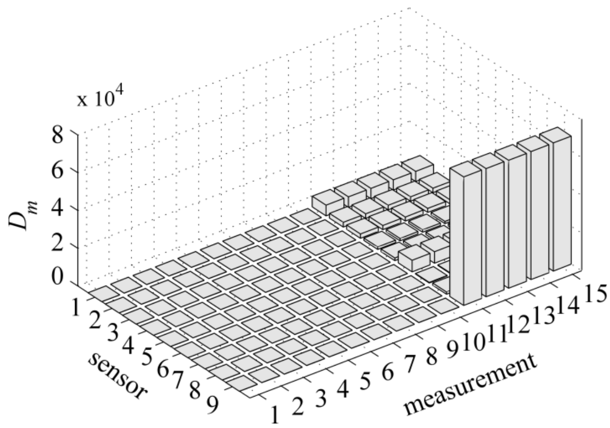

Figure 9: Results of the NSFD-Method.

4.3 Integrated Monitoring of Off-Shore Wind Energy Plants (OWEP)

Off-shore development of wind farms is attractive because the annual average wind speed is considerably higher off-shore than at most on-shore sites. To ensure a high operational reliability of future off-shore wind energy plants (OWEP) with economically acceptable repair and maintenance efforts, comprehensive diagnosis and monitoring concepts are required. Automatic monitoring systems will be an essential part of such concepts. Within the scope of the IMO-WIND research project, the German Federal Institute of Material Research and Testing (BAM), the University of Siegen and six industrial companies have been involved in developing an integrated monitoring system for the complete OWEP system including foundation, tower structure, rotor blades and machinery [90]. Operation and maintenance aspects are considered to be the main design drivers for off-shore wind farms [91]. Remote locations and poor weather conditions can postpone maintenance and result in longer downtime and greater loss of production. Therefore, the standard for off-shore reliability must be even higher than the already rigorous standards for land-based turbines. With respect to this, it becomes obvious that monitoring systems play a significant role.

Generally, off-shore wind energy plants of the multi-megawatt-class represent a huge technical challenge regarding design, construction and utilization of those structures. Concerning the acting loads and the corresponding load effects in individual structural members the state of knowledge is not sufficient. Even an economically efficient but safe foundation of offshore structures with combined actions from wind and waves is not state of the art at the present time. Because of the possibility of settlements of cyclically loaded piles in the sea bed the possibility of failure of the whole structure due to increasing fatigue or loss of stability has to be investigated [90].

Figure 10 shows a 5 MW on-shore prototype (with a rotor diameter of 116 m and height of the hub of 98 m) installed in Bremerhaven, Germany. Figure 10 gives also an impression of the tripod foundation for off-shore application.

The on-line monitoring concept for the OWEP structure is based on 3 steps. First, damage detection algorithms based on NSFD or multivariate AR models are applied to the structure of the OWEP. Since the damage detection methods are global, it is important that the output data from the accelerometers is classified by operational and environmental conditions of the OWEP. For this purpose classification techniques like *k*-means or Expectation-Maximization (EM) are used [23]. If the thresholds of damage indicators are exceeded it will be verified that no sensor fault occurred during the measurements (second step). The sensor fault identification methods, based on AR modelling or Mutual Information criterion are applied to the measured acceleration signals. If damage is discovered, the third step of the concept will be activated and a model-based algorithm for damage location is applied to the structure. The localization of damage is done by the inverse eigensensitivity method.

Figure 11 shows exemplary that the release of the nuts in one of the feet of a laboratory structure simulating the loosening of the foundation could be successfully detected and localized. Eight accelerometers have been used which were distributed along the tower. The correct location was found as the foot, with the encircled element with the lighter color in the right part of Figure 11. The procedure for model updating is very similar to the Z24-Bridge example. For lack of space the example in this chapter may give just short information about a possible strategy for monitoring of the structure of wind energy plants. The methods and the requirements on SHM systems for monitoring of wind energy plants are described in more detailed in [30]. Another important topic is the reconstruction of loads resulting from wind and waves for the purpose of updated life-time predictions, but also for design verification of the real loads [92,93,94].

Figure 10: 5 MW Multibrid 5000 off-shore wind energy plant as on-shore prototype.

5.0 CONCLUSION

This paper gave an overview on the basic principles of vibration-based methods as well as some recent developments. Applications using model-based and model-free methods have been shown. A future application of integrated monitoring of off-shore wind energy plants has been discussed. Driven by the development of advanced data processing, evaluation concepts and new sensor technologies the number of researchers in the field is still growing rapidly and the interest of the industry in the potential benefits of SHM is also large.

Although desirable, it is not always the priority to detect damage at an incipient stage. In many applications it is absolutely sufficient to be warned at an intermediate level or to only prevent catastrophic failure. The classical modal-based approach makes use of the low-frequency modes. These are global in nature which corresponds however to a reduced sensitivity. The usefulness of these methods is based on the fact that the whole structure can be monitored only by a few sensors and that the damage location needs not be known in advance. Furthermore, the use of ambient excitation often limits the frequency range. The change of the dynamic properties due to environmental changes has been recognized as a serious problem. Long-term monitoring of structures should therefore include a learning procedure how the structure behaves under certain environmental conditions to compensate these influences. Also automatic sensor fault detection is a topic of growing interest, especially in the field of aeronautics where sensors are integrated in the structure.

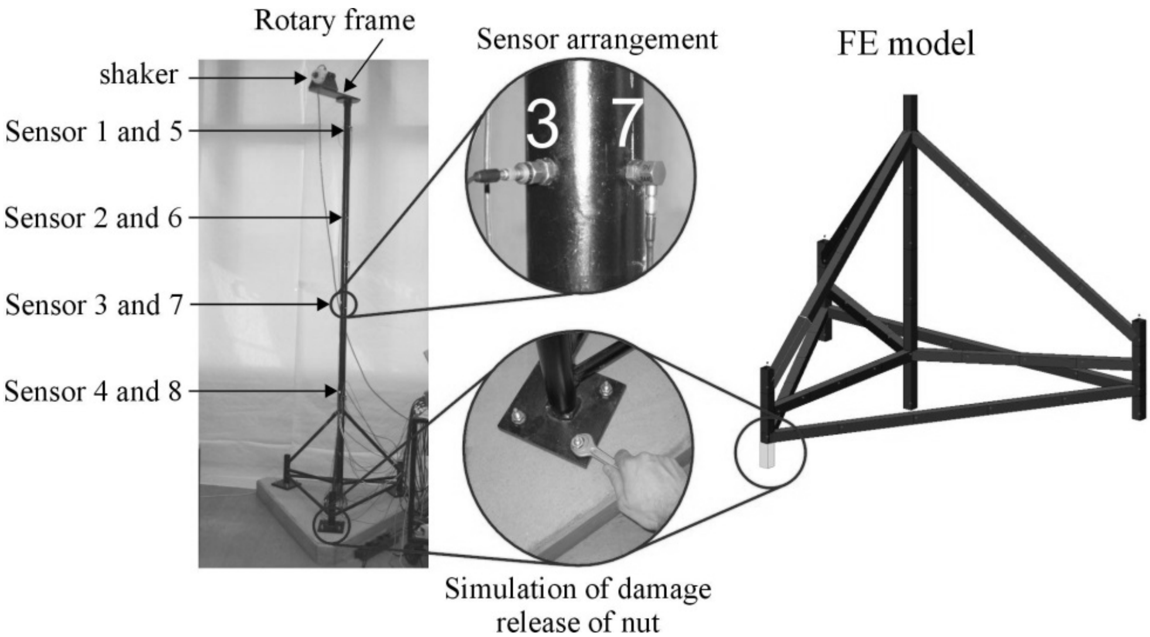

Figure 11: Damage localization on a laboratory structure.

For some applications high sensitivity might be a critical requirement. The option here is to use local methods based on ultrasonic wave propagation with one or more dense local sensor networks. To increase the sensitivity of vibration-based methods there is also a trend to develop more damage sensitive residuals and to expand the global methods into an intermediate frequency range. Modeling in the higher frequency range will become more difficult due to strong modal overlap and the complexity of mode shapes which requires also a finer sensor network. Some work should also be spent on reducing this model-dependence. To take advantage of the complementary strengths of both groups, global and local methods can be combined. Methods dealing with non-linear damage identification are not wide-spread.

The success of the SHM methods in practice will be determined by the fact whether it is possible to develop robust sensor hardware that can live as long as the monitored object. Also the decisions made by the SHM system must have a sound statistical foundation to provide reliable results. Too many false alarms as well as a missed indication of damage will destroy the confidence in such a system.

6.0 REFERENCES

1 H.J. Schmidt, J. Telgkamp, B. Schmidt-Brandecker, Application of Structural Health Monitoring to Improve Efficiency of Aircraft Structure, Proc. 2nd Europ. Workshop Structural Health Monitoring 2004, DEStech Publications, Lancaster, PA, USA, 2004, pp. 11-18.

2 A. Rytter, Vibration Based Inspection of Civil Engineering Structures, PhD Thesis, Aalborg University, Denmark, 1993.

3 H. Sohn, C.F. Farrar, F.M. Hemez, D.D. Shunk, D.W. Stinemates, B.R. Nadler and J.J. Czarnecki, A Review of Structural Health Monitoring Literature: 1996-2001, Report LA-13976-MS, Los Alamos National Laboratory, Los Alamos, NM, USA, 2004.

4 K. Worden, J.M. Dulieu-Barton., An Overview of Intelligent Fault Detection in Systems and Structures, Structural Health Monitoring, vol. 3(1), 2004, pp. 85-98.

5 D.J. Inman, C.R. Farrar, V. Lopes Jr., Steffen Jr., Damage Prognosis, Wiley&Sons, Chichester, UK, 2005.

6 C.R. Farrar, H. Sohn, F.M. Hemez, M.C. Anderson, M.T. Bement, P.J. Corwell, S.W. Doebling, J.F. Schultze, N. Lieven and A.N. Robertson, Damage Prognosis: Current Status and Future Needs, Report LA-14051-MS, Los Alamos National Laboratory, Los Alamos, NM, USA, 2003.

7 D. Balageas, C.-P. Fritzen, A. Güemes (Eds.), Structural Health Monitoring, Hermes Science Publishing, London UK, 2005.

8 D.E. Adams, Health Monitoring of Structural Materials and Components, Wiley&Sons, Chichester, UK, 2005.

9 S.W. Doebling, C.R. Farrar, M.B. Prime, D.W. Shevitz, Damage Identification and Health Monitoring of Structural Systems from Changes in Their Vibration Characteristics: A Literature Review, Report LA-12767-MS, Los Alamos National Laboratory, NM, USA, 1996.

10 C. Boller, W.J. Staszewski (Eds.), Structural Health Monitoring 2004, Proc. 2nd Europ. Workshop on Structural Health Monitoring, DEStech Publ. Lancaster, PA, USA, 2004.

11 W. Staszewski, C. Boller, G. Tomlinson (Eds.), Health Monitoring of Aerospace Structures-Smart Sensor Technologies and Signal Processing, J. Wiley & Sons, Chichester, 2004.

12 H.G. Natke C. Cempel, Model-Aided Diagnosis of Mechanical Systems, Springer, Germany, 1997.

13 K. Worden, C.R. Farrar, G. Manson, G. Park, Fundamental Axioms of Structural health Monitoring, 4th Intl. Workshop Structural Health Monitoring, Stanford University, Stanford, CA, DEStech Publ. Lancaster, PA, USA, 2005, pp. 26-41.

14 C.R. Farrar and K. Worden, An introduction to structural health monitoring, Phil. Trans. R. Soc. A (2007) 365, 303-315.

15 I. Müller, Schwingungsbasierte Schadensdiagnose delaminierter Verbundstrukturen, PhD Dissertation, University of Karlsruhe, 2005.

16 S. Seibold, C.-P. Fritzen , D. Wagner, Employing Identification Procedures for the Detection of Cracks in Rotors, Modal Analysis, vol. 11(3,4), 1996, pp. 204-215.

17 C.R. Farrar and N. Lieven, Damage Prognosis: the Future of Structural Health Monitoring, Phil. Trans. R. Soc. A (2007) 365, 623–632.

18 G. Vachtsevanos, F.L. Lewis, M. Roemer, A. Hess, B. Wu, Intelligent Fault Diagnosis and Prognosis for Engineering Systems, John Wiley and Sons, Hoboken, NJ, 2006.

19 W. Ostachowicz, M. Krawczuk, On Modelling of Structural Stiffness Loss Due to Damage, Proc. 4th Intl. Conf. On Damage Assessment of Structures: DAMAS2001, Key Engineering Materials, vols. 204-205, Transtech Pub., Switzerland, 2001, pp. 185-200.

20 H.G. Natke, Einführung in Theorie und Praxis der Zeitreihen- und Modalanalyse, Vieweg, Germany, 3rd edition, 1992.

21 M.I. Friswell, J.E. Mottershead, Finite Element Model Updating in Structural Dynamics, Kluwer Academic Publishers, 1995.

22 H. Sohn, C.R. Farrar, N.F. Hunter, K. Worden, Structural Health Monitoring Using Statistical Pattern Recognition Techniques, Journal Dynamic Systems, Meas. And Control, Transaction of the ASME, vol. 123, 2001, pp. 706-711.

23 C.M. Bishop, Neural Networks for Pattern Recognition, Oxford Univ. Press, Oxford, 1995.

24 C.R. Farrar, K. Worden, Structural Health Monitoring-A Machine Learning Perspective, Wiley, 2013.

25 D.-A. Tibaduiza, M.-A. Torres-Arredondo, L.E. Mujica, J. Rodellar, C.-P. Fritzen, A study of two unsupervised data driven statistical methodologies for detecting and classifying damages in structural health monitoring, MSSP Vol. 41, Issues 1–2, pp. 467-484, 2013.

26 M.A. Torres-Arredondo, D.A. Tibaduiza, D-A., M. McGugan, H.L.Toftegaard, K.K. Borum, L. Mujica, Rodellar, J.,C.-P. Fritzen, Multivariate data-driven modelling and pattern recognition for damage detection and identification for acoustic emission and acousto-ultrasonics. *Smart Materials and Structures*, *22*, [105023]. doi: 10.1088/0964-1726/22/10/105023, 2013.

27 M. A. Torres-Arredondo, D.A. Tibaduiza, L.E. Mujica, J. Rodellar, C.-P. Fritzen, Data-driven multivariate algorithms for damage detection and identification: Evaluation and comparison, Structural Health Monitoring, Vol. 13, 1: pp. 19-32., 2014.

28 I. Buethe, P. Kraemer, C.-P. Fritzen, Applications of Self-Organizing Maps in Structural Health Monitoring. Key Engineering Materials, 518, 37-46, 2012.

29 C.-P. Fritzen, G. Mengelkamp, A. Güemes, Elimination of Temperature Effects on Damage Detection within a Smart Structure Concept, Proc. 4th International Workshop on Structural Health Monitoring, Stanford University, USA, 15-17 Sept 2003, pp. 1530-1538.

30 P. Kraemer, C.-P. Fritzen, Concept for Structural Damage Identification of Offshore Wind Energy Plants, Proc. 6th International Workshop on Structural Health Monitoring, Stanford University, USA, 11-13 Sept 2007, pp. 1881-1888.

31 H. Sohn, K. Worden, C.R. Farrar, Statistical Damage Classification Under Changing Environmental and Operational Conditions, Journal of Intelligent Material Systems and Structures, 13, 2002, pp. 561-574.

32 J. Kullaa, Damage Detection under a Varying Environment using the Missing Data Concept, Proc. 5th International Workshop on SHM, Stanford University, USA, 12-14 Sept. 2005, pp. 565-573.

33 J. Kullaa, Elimination of Environmental Influences from Damage-Sensitive Features in a Structural Health Monitoring System, Proc. of 1st European Workshop on SHM, Paris, 2002, pp.742–749.

34 V. Lämsä, J. Kullaa, Nonlinear Factor Analysis in Structural Health Monitoring to Remove Environmental Effects, Proc. 6th International Workshop on Structural Health Monitoring, Stanford University, USA, 11-13 Sept, 2007, pp. 1092-1099.

35 A.-M. Yan, G. Kerschen, P. De Boe, J.-C. Golinval, Structural damage diagnosis under varying environmental conditions - part 2: local PCA for non-linear cases, Mechanical Systems and Processing, 19, 2005, pp. 865-880.

36 H. Sohn, Effects of environmental and operational variability on structural health monitoring, Phil. Trans. R. Soc. A, 2007, 365, pp. 539-560.

37 C.-P. Fritzen, P. Kraemer, I. Buethe, Vibration-based Damage Detection under Changing Environmental and Operational Conditions. Advances in Science and Technology, 83, pp 95-104, 2013.

38 C. Papadimitriou, J.L. Beck, S.-K. Au, Entropy-based Optimal sensor Location for Structural Model Updating, Journal of Vibration and Control, Vol. 6, 2000, pp. 781-800.

39 R.T. Schulte, K. Bohle, C.-P. Fritzen, G. Schuhmacher, Optimal Sensor Placement for Damage Identification-An Efficient Forward-Backward Selection Algorithm, Proc. 3. EWSHM, Granada, Spain, 2006, pp. 1151-1159.

40 K. Bohle, Sensitivitätsbasierte Methoden zur modellgestützten Schadendiagnose mit Modaldaten, PhD Dissertation, University of Siegen, 2005.

41 D.S. Li, Sensor Placement methods and Evaluation Criteria in Structural Health Monitoring, PhD Dissertation, Univ. of Siegen, 2011.

42 D.S. Li, H.N. Li, C.-P. Fritzen, On Optimal Sensor Placement Criterion for Structural Health Monitoring with Representative Least Squares Method, Key Engineering Materials, Vols. 413-414, pp. 383.391, 2009.

43 I. Trendafilova, W. Heylen, Measurement point selection in damage detection using the average mutual information, Europ. COST F3 Conference on System Identification & SHM, Madrid, Vol. 1, 2000, pp. 147-156.

44 R. Dunia, S. J. Qin, T. F. Edgar, T. J. McAvoy, Identification of faulty sensors using principal component analysis, AiChe Journal, Vol. 42, No. 10, 1996, pp. 2797-2812.

45 G. Kerschen, P. De Boe, J.-C. Golinval, K. Worden, Sensor validation for on-line vibration monitoring, Proc. 2nd Europ. Workshop on Structural Health Monitoring 2004, C. Boller and W.J. Staszewski (editors), Munich, Germany, DEStech Publications, (July 7-9, 2004), pp. 819-827.

46 D. L. Mattern, L. C. Jaw, T.-H. Guo, R. Graham, W. McCoy, Using Neural Network for Sensor Validation, 34th Joint Propulsion Conference cosponsored by AIAA, ASME, SAE and ASEE, Cleveland, Ohio, USA (July 12-15, 1998).

47 K. Worden, Sensor validation and correction using auto-associative neural networks and principal component analysis, Proc. IMAC XXI, Orlando, USA, 2003.

48 J. Kullaa, Sensor fault identification and correction in structural health monitoring, Proc. 6th International Workshop on Structural Health Monitoring, Stanford University, USA, 2007, pp. 606-613.

49 P. Kraemer, C.-P. Fritzen, Sensor Fault Identification Using Autoregressive Models and the Mutual Information Concept, DAMAS 2007, Torino, Italy, Key Engineering Materials, vol. 347, 2007, pp. 387-392.

50 G. Park, C.R. Farrar, F. Lanza di Scalea, S. Coccia, Performance assessment and validation of piezoelectric active-sensors in structural health monitoring, Smart Materials and Structures, Vol. 15, 2006, pp. 1673-1683.

51 B. Weber, P. Paultre, J. Proulx, Damage Detection of Aluminium Truss Using Tikhonov Regularization, Proc. XXIV. IMAC, Jan 30-Feb 2, 2006, St. Louis, MO, USA, on CD Rom, ISBN 0-912053-94-1.

52 M. Link, S. Stöhr, M. Weiland, Identification of Structural Property Degradations by Computational Model Updating, Key Engineering Materials, Vol. 347 (2007), pp. 19-34.

53 C.-P. Fritzen, D. Jennewein, T. Kiefer, Damage Detection Based on Model-Updating Methods," Mechanical Systems & Signal Processing, 12(1), 1998, pp. 163-186.

54 C.-P. Fritzen, K. Bohle, Parameter selection strategies in model-based damage detection, Structural Health Monitoring 2000, Technomic Publishing., Lancaster, PA, USA, 1999, pp. 901-911.

55 D.J. Ewins, Modal Testing: Theory and Practice, Research Study Press, UK, 2000.

56 W. Heylen, S. Lammens, P. Sas, Modal Analysis Theory and Testing, Kath. Universiteit Leuven, Leuven, Belgium, 1998.

57 B. Peeters, G. De Roeck, Reference-Based Stochastic Subspace Identification for Output-Only Modal Analysis, Mechanical Systems and Signal Processing, 13(6), 1999, pp. 855-878.

58 B. Peeters, G. De Roeck, Stochastic system identification for operational modal analysis: A review, J. Dynamic Systems, Measurement and Control, vol.123, 2001, pp. 659-667.

59 P. Cawley, R.D. Adams, The location of defects in structures from measurements of natural frequencies, J. Strain Analysis, vol. 14, 1979, pp.49–57.

60 D.C. Zimmerman, M. Kaouk, Structural Damage Detection Using a Minimum Rank Update Theory, Journal of Vibration and Acoustics, 116(2), 1994, pp. 222-231.

61 D.C. Zimmerman, Looking into the Crystal Ball: The Continued Need for Multiple Viewpoints in Damage Detection, Damage Assessment of Structures, M.D. Gilchrist, J.M. Dulieu-Barton and K. Worden, Trans Tech Publications, 1999, pp. 76-90.

62 N. Stubbs, J.-T. Kim, C.R. Farrar, Field Verification of a Nondestructive Damage Localization and Severity Estimation Algorithm, Proc. 13th Intl. Modal Analysis Conference, Nashville, TN, USA, 1995, pp. 210-218.

63 J. Maeck, Damage Assessment of Civil Engineering Structures by Vibration Monitoring, PhD-Dissertation, KU Leuven, Leuven, Belgium, 2003.

64 P. Ladeveze, M. Reynier, A Localization Method of Stiffness Errors for the Adjustment of FE Models, Proc. 12th ASME Conf. on Mech. Vibr. and Noise, Montreal, Canada (ASME), 1989, pp. 355-361.

65 C.-P. Fritzen, K. Bohle, Damage Identification using a Modal Kinetic Energy Criterion and Output-Only Modal Data-Application to the Z-24 Bridge, Proc. 2nd European Workshop Structural Health Monitoring, Munich, Germany, DEStech Publ. Lancaster, PA, USA, 2004, pp. 185-194.

66 M. Oeljeklaus, Projection Methods within Model Updating, Inverse Problems in Engineering, vol. 8, 2000, pp. 119-141.

67 D. Otte, H. van der Auweraer, J. Leuridan, The Use of Multivariate Correlation Techniques For Vibro-Acoustic Experimental Data Analysis, Proc. 17th Intl. Seminar on Modal Analysis, Course on Advanced Techniques in Applied Acoustics, KU Leuven, Belgium, 1992.

68 T.J. Johnson, D.E. Adams, Transmissibility as a Differential Indicator of Structural Damage, J. Vibration and Acoustics, vol. 124, 2002, pp. 634-641.

69 R.P.C. Sampaio, N.M.M. Maia, J.M.M. Silva, A.M.R. Ribeiro, On the Use of Transmissibility for Damage Detection and Localization, Proc. Europ. Cost F3 Conf. System Ident. & Struct. Health Monitoring, vol. 1, University of Madrid, Spain, 2000, pp.363-376.

70 G. Hilson, K. Worden , G. Manson, Feature Selection for a Neural Damage Locator Using a Genetic Algorithm, Proc. 2nd Europ. Workshop on Structural Health Monitoring, Paris, France, DEStech Publ., Lancaster, PA, USA, 2004, pp. 624-632.

71 C. Liang, F.P. Sun, C.A. Rogers, Coupled Electro-Mechanical Analysis of Adaptive Material Systems - Determination of the Actuator Power Consumption and System Energy Transfer, Journal of Intelligent Materials and Structures, Vol. 5(1), pp. 12-19, 1994.

72 G. Park, H. Sohn, C.F. Farrar, D.J. Inman, Overview of Piezoelectric Impedance-Based Health Monitoring and Path Forward, The Shock and Vibration Digest, 35(6), 2003, pp. 451-463.

73 V. Giurgiutiu, Lyshewski, S.E., Micromechatronics, CRC Press, Boca Raton, 2004.

74 V. Giurgiutiu, Structural Health Monitoring with Piezoelectric Wafer Active Sensors, Elsevier, 2008.

75 I. Buethe, B. Eckstein, C.-P. Fritzen, Model-based Detection of Sensor Faults under Changing Temperature Conditions, Structural Health Monitoring, published online, doi: 10.1177 /1475921713510755, 2013.

76 I. Buethe, C.-P. Fritzen, Sensor Performance Assessment Based on a Physical Model and Impedance Measurements. Key Engineering Materials, 569-570, 751-758, 2013.

77 J.J. Gertler, Fault Detection and Diagnosis in Engineering Systems, Marcel Dekker, Inc., New York, Basel, Hong Kong, 1998.

78 S.D. Fassois, J.S. Sakellariou, Time series methods for fault detection and identification in vibrating structures, Phil. Trans. R. Soc., 365, 2007, pp. 411-448.

79 M. Basseville, M. Abdelghani, A. Benveniste, Subspace-based fault detection algorithms for vibration monitoring, Automatica, vol. 36, 2000, pp. 101-109.

80 M. Basseville, A. Benveniste, M. Goursat, L. Hermans, L. Mevel , H. van der Auweraer, Output-Only Modal Subspace-Based Structural Identification: From Theory to Industrial Testing Practice, Journal Dynamic Systems, Measurement and Control, vol. 123, 2001, pp. 668-676.

81 C.-P. Fritzen, G. Mengelkamp, A. Güemes, A CFRP Plate with Piezo-Electric Actuators and Sensors as Self-Diagnostic Intelligent Structure, Proc. ISMA 2002, KU Leuven, Belgium, 2002, pp. 185-191.

82 C.-P. Fritzen, G. Mengelkamp, A. Güemes, Detection of Small Delaminations in a CFRP Plate by Vibration-Based Structural Health Monitoring, Proc. 14th. Intl. Conf. on Composite Materials, San Diego, 2003, pp.110-121.

83 Y. Aimin, J.-C. Golinval, F. Marin, Fault Detection Algorithm based on Null-Space Analysis for On-line Structural Health Monitoring, Proc. 23rd IMAC, Jan. 31- Feb. 2, Orlando, FL, Soc. Exp. Mechanics, published on CD-ROM, 2005.

84 R.K. Mehra, J. Peschon, 1971, An Innovations Approach to Fault Detection and Diagnosis in Dynamic Systems, Automatica, vol. 7, pp. 637-640.

85 C.-P. Fritzen, G. Mengelkamp, A Kalman Filter Approach to the Detection of Structural Damage, Proc. 4th Intl. Workshop Structural Health Monitoring, Stanford University, Stanford, CA, DEStech Publ. Lancaster, PA, USA., 2003, pp.1275-1284.

86 J. Maeck, G. De Roeck, Description of Z24-benchmark, MSSP, 17(1), 2003, pp. 127-132.

87 J. Maeck, B. Peeters and G. De Roeck, Damage identification on the Z24-bridge using vibration monitoring analysis. Smart Materials and Structures, Smart Materials and Structures, 10(3), 2001, pp.512-517.

88 J. Maeck, G. De Roeck, Damage assessment using vibration analysis on the Z24-bridge, MSSP, 17(1), 2003, pp. 133-142.

89 C.-P. Fritzen, P. Kraemer, K.J. Xing, Damage Detection and Localization using Time Domain Residuals, Proc. World Forum on Smart Materials and Smart Structures Technology (SMSST'07), Chongqing & Nanjing, P.R. China, May 22-27, 2007 (on CD-ROM).

90 R. Rohrmann, W. Ruecker, IMO-Wind: An Integrated Monitoring System for Offshore Wind Energy Turbines, Proc. Eurodyn 2005, September 2005, Paris, France.

91 R. Gasch, J. Twele, Wind Power Plants, Solarpraxis Berlin, James & James, London, 2002.

92 M. Klinkov, C.-P. Fritzen, Online Force Reconstruction Using Robust Observers, EWSHM'06 Proceeding, Spain, 5-7 July 2006, paper no. 76 on CD-ROM..

93 C.-P. Fritzen and M. Klinkov, Online Wind Load Estimation for Offshore Wind Energy Plants, Proc. 6th International Workshop on Structural Health Monitoring, Stanford University, USA, 11-13 Sept, 2007, pp. 1905-1912.

94 C.-P. Fritzen, M. Klinkov, P. Kraemer: Vibration-based Damage Diagnosis and Monitoring of External Loads, in Ostachowicz W., Guemes, A (Eds.) New Trends in Structural Health Monitoring, CISM Lecture Notes No. 542, Springer, pp. 149-208, 2013.